Supplementary Materials

Reductive O-formylation of carbon dioxide and alcohols over porous phenanthroline-based polymer supported single iridium atom catalyst

Kang Zhao[1], Dongcheng He[1], Hongyan Ni[1,2], Hongli Wang[1], Ce Liu[1], Dongyuan Yang[3], Xionghou Gao[4], Junyi Zhang[4], Honghai Liu[5], Xinjiang Cui[1,*], Feng Shi[1,*]

[1]State Key Laboratory of Low Carbon Catalysis and Carbon Dioxide Utilization, State Key Laboratory for Oxo Synthesis and Selective Oxidation, Lanzhou Institute of Chemical Physics, Chinese Academy of Sciences, Lanzhou 730000, Gansu, China.
[2]University of Chinese Academy of Sciences, Beijing 100049, China.
[3]School of Chemistry and Chemical Engineering, Xi'an University of Science and Technology, Xi'an 710054, Shaanxi, China.
[4]PetroChina Lanzhou Petrochemical Company, Lanzhou 730060, Gansu, China.
[5]Petrochina Lanzhou Chemical Research Center, Lanzhou 730060, Gansu, China.

[*]**Correspondence to:** Prof. Xinjiang Cui, Prof. Feng Shi, State Key Laboratory of Low Carbon Catalysis and Carbon Dioxide Utilization, State Key Laboratory for Oxo Synthesis and Selective Oxidation, Lanzhou Institute of Chemical Physics, Chinese Academy of Sciences, Lanzhou 730000, Gansu, China. E-mail: xinjiangcui@licp.cas.cn; fshi@licp.cas.cn

Contents

1. General Information

Chemicals and materials

All solvents and chemicals, unless otherwise noted, were obtained commercially and were used as received without further purification. All glassware was dried before using. Analytical thin layer chromatography (TLC) was performed using pre-coated Jiangyou silica gel HSGF254 (0.2mm±0.03mm). Flash chromatography was performed using silica gel 60, 0.063-0.2 mm, 200-300 mesh (Jiangyou, Yantai) with the indicated solvent system.

Instrumental measurements and physical characterization

Gas chromatography analysis was performed on Agilent 7890A GC equipped with a HP-5 capillary column and FID detector. GC-MS analysis was in general recorded on an Agilent 5977A MSD GC-MS.

High resolution mass spectra were recorded on a Bruker Q-TOF II MSD.

The contents of Rh in the catalysts were measured by inductively coupled plasma-atomic emission spectrometry (ICP-AES), using Iris advantage Thermo Jarrel Ash device.

Fourier transform infrared (FT-IR) spectrum were recorded with a Bruker VERTEX 70FTIR spectrometer.

The liquid nuclear magnetic resonance spectra (NMR) were recorded on a Bruker AvanceTM III 400 MHz in deuterated chloroform unless otherwise noted. Data are reported in parts per million (ppm) as follows: chemical shift, multiplicity (s = singlet, d = doublet, t = triplet, q = quartet, quint = quintet, m = multiplet, dd = doublet of doublet and br = broad signal), coupling constant in Hz and integration.

Powder X-ray diffraction (PXRD) measurements were conducted were conducted by a STADIP automated transmission diffractometer (STOE) equipped with an incident beam curved germanium monochromator selecting CuKα1 radiation and a 6° position sensitive detector (PSD) (step size: 0.014^{o}, step time: 25.05 s). The XRD patterns were scanned in the 2θ range of 5-80°.

Nitrogen adsorption-desorption isotherms were measured at 77 K using an American Quantachrome iQ$_2$ automated gas sorption analyzer. The samples were outgassed at 120 ^{o}C for 12 h before the measurements. Surface areas were calculated from the adsorption data using Langmuir and Brunauer-Emmett-Teller (BET) methods. The pore-size-distribution curves were obtained from the adsorption branches using non-local density functional theory (NLDFT) method.

X-ray photoelectron spectroscopy (XPS) measurements were carried out by a VG ESCALAB 210 instrument equipped with a dual Mg/Al anode X-ray source, a hemispherical capacitor analyzer, and a 5 keV Ar^{+} ion gun. All spectra were recorded by using AlKa (1361 eV) radiation. The electron binding energy was referenced to the C1s peak at 284.8 eV.

The thermal properties of Rh@POPs catalysts were evaluated using a METTLER TOLEDO simultaneous thermal analyzer over the temperature range from 30 to 800 °C under nitrogen atmosphere (20 mL/min) with a heating rate of 5 °C/min.

Field emission scanning electron microscopy (SEM) observations were performed on a Hitachi S-4800 microscope operated at an accelerating voltage of 5.0 kV.

High-resolution transmission electron microscope (HR-TEM) analysis was carried out on a Talos F200S operating at 200 kV.

The abreaction-corrected HAADF-STEM images were acquired using a Thermo Fisher Spectra 300 transmission electron microscope equipped with probe and imaging spherical aberration correctors, and with high voltage of 300kV.

The XAFS spectra were recorded at room temperature using a 4-channel Silicon Drift Detector (SDD) Bruker 5040. Ir K-edge analysis was performed with Si(111) crystal monochromators at the BL11B beamlines at the Shanghai Synchrotron Radiation Facility (SSRF) (Shanghai, China). Before the analysis at the beamline, samples were pressed into thin sheets with 1 cm in diameter and sealed using Kapton tape film. Ir K-edge extended X-ray absorption fine structure (EXAFS) spectra were recorded in transmission mode. Negligible changes in the line-shape and peak position of Ir K-edge XANES spectra were observed between two scans taken for a specific sample. The XAFS spectra of these standard samples (Ir foil, $IrCl_3$, and IrO_2) were recorded in transmission mode. The spectra were processed and analyzed by the software codes Athena.

2. Synthesis of 3,8-diviny-1,10-phenanthroline and tris(4-vinylphenyl)amine.

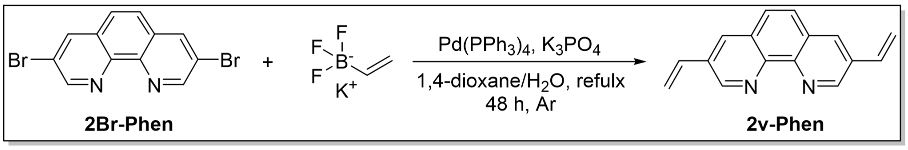

3,8-dibromo-1,10-phenanthroline (5.10 g, 15 mmol), potassium vinyltrifluoroborate (6.03 g, 45 mmol), $Pd(PPh_3)_4$ (516 mg), K_3PO_4 (19.2 g, 90 mmol), 1,4-dioxane (90 mL), and H_2O (30 mL) were mixed under Ar and refluxed for 48 h. After cooling down to room temperature, the reaction mixture was extracted with CH_2Cl_2 (3×100 mL). The combined organic phase was washed with brine, dried over Na_2SO_4, and evaporated in vacuum. The product was purified by flash column chromatography over silica gel (CH_2Cl_2/hexane/triethylamine at 40/50/10) to give 3,8-diviny-1,10-phenanthroline as a light yellow solid (3.13 g, 90%).[1]

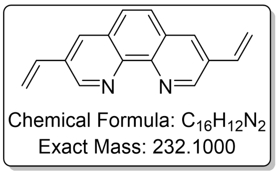

3,8-divinyl-1,10-phenanthroline: yellow solid, 3.13 g, 90% yield. **^{1}H NMR** (400 MHz, $CDCl_3$) δ 9.13 (d, J = 1.6 Hz, 2H), 8.01 (d, J = 1.7 Hz, 2H), 7.59 (s, 2H), 6.83 (dd, J = 17.6, 11.0 Hz, 2H), 5.96 (d, J = 17.7 Hz, 2H), 5.43 (d, J = 11.0 Hz, 2H). **^{13}C NMR** (101 MHz, $CDCl_3$) δ 148.92, 145.32, 133.44, 132.17, 132.00, 128.27, 126.81, 117.16, 77.16. **HRMS** (ESI): Calcd. for $C_{16}H_{13}N_2$ $[M+H]^+$: 233.1073, found: 233.1074.

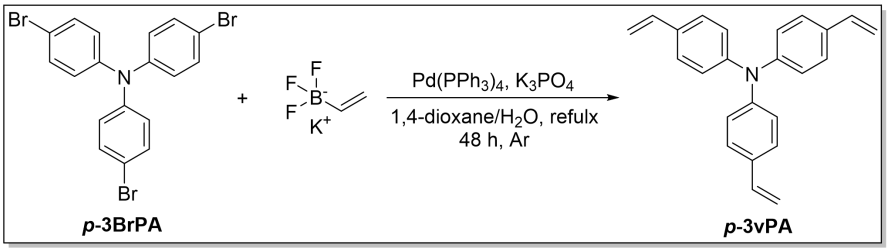

p-3BrPA (1.20 g, 2.5 mmol), potassium vinyltrifluoroborate (1.51 g, 11.25 mmol), $Pd(PPh_3)_4$ (130 mg), K_3PO_4 (4.77 g, 22.5 mmol), 1,4-dioxane (22.5 mL), and H_2O (7.5 mL) were mixed under Ar and refluxed for 48 h. After cooling down to room temperature, the reaction mixture was extracted with CH_2Cl_2 (3×30 mL). The combined organic phase was washed with brine, dried over Na_2SO_4, and evaporated in vacuum. The product was purified by flash column chromatography over silica gel (PE as the eluent) to give *p*-3vPA as a white solid (0.242 g, 30%).

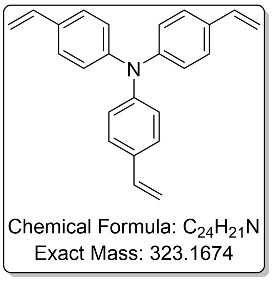

Tris(4-vinylphenyl)amine: white solid, 0.242 g, 30% yield. ^{1}**H NMR** (400 MHz, $CDCl_3$) δ 7.28 (d, *J* = 8.6 Hz, 6H), 7.03 (d, *J* = 8.6 Hz, 6H), 6.65 (dd, *J* = 17.6, 10.9 Hz, 3H), 5.64 (dd, *J* = 17.6, 0.7 Hz, 3H), 5.24 – 4.85 (m, 3H).

^{13}**C NMR** (101 MHz, $CDCl_3$) δ 147.08, 136.28, 132.49, 127.26, 124.18, 112.56.

3. Synthetic procedure of the porous phenanthroline-based polymer catalysts

Preparation of the POP-Phen

0.80 g of 2v-Phen was dissolved in 8 mL of DMF, followed by the addition of 20 mg of AIBN. The mixture was transferred into an autoclave, stirred at room temperature for 0.5 h, and then heated to 100 °C for 24 h without stirring. After the polymerization was finished, the resulting solid was filtered, washed with THF (20 ml×3) and Et_2O (20 ml×3), and dried under vacuum at room temperature. Finally, the POP-Phen was obtained as a yellow solid.

Preparation of the M/POP-Phen

As a typical run, 0.16 g of POP-Phen was swelled in 3 mL of DMF for 1 h, followed by dropwise adding the Ir solution (32 mg of $IrCl_3 \cdot 3H_2O$ dissolved in 3 mL of DMF) under vigorous stirring. The mixture continued to stir at room temperature for 24 h. After the immobilization of Ir was finished, the resulting solid was filtered, washed with THF (20 ml×3) and Et_2O (20 ml×3), and dried under vacuum at room temperature. Finally, the Ir/POP-Phen was obtained as a brown solid. Other kinds of POP-Phen supported metal catalysts were obtained by replacing 32 mg of $IrCl_3 \cdot 3H_2O$ with 26 mg of $Pd(CH_3CN)_2$, 26 mg of $RhCl_3 \cdot 3H_2O$, 41 mg of H_2PtCl_4, 34 mg of $HAuCl_4$, 27 mg of $RuCl_3 \cdot 3H_2O$, 34 mg of $CuCl_2 \cdot 2H_2O$, 24 mg of $CoCl_2 \cdot 6H_2O$, 17 mg of $AgNO_3$, or 24 mg of $NiCl_2 \cdot 6H_2O$, respectively, and denoted as the M/POP-Phen.

Preparation of the Ir/POP-Phen-$NaBH_4$

80 mg of the Ir/POP-Phen was dispersed in 8 mL of MeOH, then 76 mg of $NaBH_4$ was slowly added under vigorous stirring. The mixture was reacted at room temperature for 3 h. After the reduction process, the solid catalyst was filtered, washed with MeOH (20 ml×3) and Et_2O (20 ml×3), and dried under vacuum at room temperature. Finally, the Ir/POP-Phen-$NaBH_4$ was obtained as a dark solid.

Preparation of the Ir@POP-Phen

0.16 g of 2v-Phen and 32 mg of $IrCl_3 \cdot 3H_2O$ were dissolved in 2 mL of DMF, followed by the addition of 4 mg of AIBN. The mixture was transferred into an autoclave, stirred at room temperature for 0.5 h, and then heated to 100 °C for 24 h without stirring. After the polymerization was finished, the resulting solid was filtered, washed with THF (10 ml×3) and Et_2O (10 ml×3), and dried under vacuum at room temperature. Finally, the Ir@POP-Phen was obtained as a brown solid.

Preparation of the Ir/POP-Phen&DVB

47 mg of 2v-Phen and 129 mg of divinylbenzene (DVB) were dissolved in 2 mL of DMF, followed by the addition of 5 mg of AIBN. The mixture was transferred into an autoclave, stirred at room temperature for 0.5 h, and then heated to 100 °C for 24 h without stirring. After the polymerization was finished, the resulting solid was filtered, washed with THF (10 ml×3) and Et_2O (10 ml×3), and dried under vacuum at room temperature.

The above obtained POP-Phen&DVB was swelled in 3 mL of DMF for 1 h, followed by dropwise adding the Ir solution (32 mg of $IrCl_3 \cdot 3H_2O$ dissolved in 3 mL of DMF) under vigorous stirring. The mixture continued to stir at room temperature for 24 h. After the immobilization of Ir was finished, the resulting solid was filtered, washed with THF (20 ml×3) and Et_2O (20 ml×3), and dried under vacuum at room temperature. Finally, the Ir/POP-Phen&DVB was obtained as a brown solid.

Preparation of the Ir/POP-Phen&*p*-3vPA

47 mg of 2v-Phen and 129 mg of *p*-3vPA were dissolved in 2 mL of DMF, followed by the addition of 5 mg of AIBN. The mixture was transferred into an autoclave, stirred at room temperature for 0.5 h, and then heated to 100 °C for 24 h without stirring. After the polymerization was finished, the resulting solid was filtered, washed with THF (10 ml×3) and Et_2O (10 ml×3), and dried under vacuum at room temperature.

The above obtained POP-Phen&*p*-3vPA was swelled in 3 mL of DMF for 1 h, followed by dropwise adding the Ir solution (32 mg of $IrCl_3 \cdot 3H_2O$ dissolved in 3 mL of DMF) under vigorous stirring. The mixture continued to stir at room temperature for 24 h. After the immobilization of Ir was finished, the resulting solid was filtered, washed with THF (20 ml×3) and Et_2O (20 ml×3), and dried under vacuum at room temperature. Finally, the Ir/POP-Phen&*p*-3vPA was obtained as a brown solid.

4. Experimental procedure for the O-formylation of alcohols

For *n*-BuOH substrate: the as-prepared Ir/POP-Phen catalyst (1.9 mg containing 0.83 μmol of Ir), *n*-BuOH (48 mL), Et_3N (20 mL) were added into a 140 ml stainless-steel autoclave with a magnetic stir bar. After the autoclave was sealed and purged with 1 MPa of CO_2 for four times, the pressure of CO_2 was adjusted to 4 MPa and kept at this pressure for 5 min, then another 6 MPa of H_2 was introduced. So total pressure in the autoclave was 10 MPa at room temperature. The autoclave was put into a preheated reactor, and stirring at 160 °C for 48 h. After the reaction, the autoclave was cooled to room temperature and the pressure was carefully released. Subsequently, the reaction mixture was diluted with ethyl acetate (8 ml), the solid catalyst was removed from the system by centrifugation. The liquid was subjected to gas chromatography analysis (Agilent 7890A GC equipped with a HP-5 capillary column with 5 wt.% phenyl groups and the FID detector) to determine the yield, TON, and TOF by using *m*-xylene as the internal standard.

Optimization of different parameters for O-formylation of *n*-BuOH was varied according to the actual reaction demand, see the reaction condition optimization section in the manuscript and Supporting Information for detailed reaction parameters.

For recycling: the as-prepared Ir/POP-Phen catalyst (38 mg containing 16.6 μmol of Ir), *n*-BuOH (48 mL), Et_3N (20 mL) were added into a 140 ml stainless-steel autoclave with a magnetic stir bar. After the autoclave was sealed and purged with 1 MPa of CO_2 for four times, the pressure of CO_2 was adjusted to 4 MPa and kept at this pressure for 5 min, then another 6 MPa of H_2 was introduced. So total pressure in the autoclave was 10 MPa at room temperature. The autoclave was put into a preheated reactor, and stirring at 160 °C for 12 h. After the reaction, the autoclave was cooled to room temperature and the pressure was carefully released. Subsequently, the reaction mixture was diluted with ethyl acetate (8 ml), the solid catalyst was removed from the system by centrifugation. The liquid was subjected to gas chromatography analysis (Agilent 7890A GC equipped with a HP-5 capillary column with 5 wt.% phenyl groups and the FID detector) to determine the yield, TON, and TOF by using *m*-xylene as the internal standard.

The spent Ir/POP-Phen catalyst was washed with MeOH (8.0 ml×3) and THF (8.0 ml×3), and dried at 60 °C under vacuum. Then the spent Ir/POP-Phen catalyst was used for next run. The Ir contents of the reused catalyst and filtrate after each run were determined by inductively coupled plasma-atomic emission spectrometry (ICP-AES).

For MeOH substrate: the as-prepared Ir/POP-Phen catalyst (1.9 mg containing 0.83 μmol of Ir), MeOH (48 mL), Et_3N (20 mL) were added into a 140 ml stainless-steel autoclave with a magnetic stir bar. After the autoclave was sealed and purged with 1 MPa of CO_2 for four times, the pressure of

CO_2 was adjusted to 4 MPa and kept at this pressure for 5 min, then another 6 MPa of H_2 was introduced. So total pressure in the autoclave was 10 MPa at room temperature. The autoclave was put into a preheated reactor, and stirring at 160 °C for 48 h. After the reaction, the autoclave was cooled by freezing and the pressure was carefully released. Subsequently, the reaction mixture was diluted with MeOH (8 ml), the solid catalyst was removed from the system by centrifugation. The liquid was subjected to gas chromatography analysis (Agilent 7890A GC equipped with a HP-5 capillary column with 5 wt.% phenyl groups and the FID detector) to determine the yield, TON, and TOF by using 1,4-dioxane as the internal standard.

For EtOH and *n*-PrOH substrates: the as-prepared Ir/POP-Phen catalyst (1.9 mg containing 0.83 μmol of Ir), alcohol (48 mL), Et_3N (20 mL) were added into a 140 ml stainless-steel autoclave with a magnetic stir bar. After the autoclave was sealed and purged with 1 MPa of CO_2 for four times, the pressure of CO_2 was adjusted to 4 MPa and kept at this pressure for 5 min, then another 6 MPa of H_2 was introduced. So total pressure in the autoclave was 10 MPa at room temperature. The autoclave was put into a preheated reactor, and stirring at 160 °C for 48 h. After the reaction, the autoclave was cooled by freezing and the pressure was carefully released. Subsequently, the reaction mixture was diluted with ethyl acetate (8 ml), the solid catalyst was removed from the system by centrifugation. The liquid was subjected to ^1H NMR analysis to determine the yield, TON, and TOF by using 1,3,5-Trimethoxybenzene as the internal standard.

For other alcohol substrates: the as-prepared Ir/POP-Phen catalyst (1.9 mg containing 0.83 μmol of Ir), alcohol (48 mL), Et_3N (20 mL) were added into a 140 ml stainless-steel autoclave with a magnetic stir bar. After the autoclave was sealed and purged with 1 MPa of CO_2 for four times, the pressure of CO_2 was adjusted to 4 MPa and kept at this pressure for 5 min, then another 6 MPa of H_2 was introduced. So total pressure in the autoclave was 10 MPa at room temperature. The autoclave was put into a preheated reactor, and stirring at 160 °C for 48 h. After the reaction, the autoclave was cooled to room temperature and the pressure was carefully released. Subsequently, the reaction mixture was diluted with ethyl acetate (8 ml), the solid catalyst was removed from the system by centrifugation. The liquid was subjected to ^1H NMR analysis to determine the yield, TON, and TOF by using 1,3,5-Trimethoxybenzene as the internal standard.

5. Reaction performance comparison between the precedent and our work

Supplementary Table 1. Reaction performance comparison between the previously reported homogeneous catalysts and the Ir/POP-Phen catalyst

Entry	**Cat.**	**CO_2/H_2 (MPa)**	**T (^oC)**	**t (h)**	**TON**	**TOF (h^{-1})**	**Ref.**
1	$RuHCl(dppm)_2$	4.5/1.5	140	20	664	33	[2]
2	Ru complex-1	5/8.5	65	3.9	5480	1400	[3]
3	Ru complex-2	2/9	90	18	1290	72	[4]
4	Ru complex-3	3/9	60	64	9542	149	[5]
5	$RuCl_2(PPh_3)_3$	0.1/2	140	40	5000	125	[6]
6	Ru/L14	3/3	100	20	4126	206	[7]
7	Fe/L2	3/3	100	20	1692	85	[8]
8	$Co(BF_4)_2 \cdot 6H_2O$+tetraphos	3/6	100	20	659	22	[9]
9	Ru complex-4	1/3	135	16	40	2.5	[10]
10	$[FeH(PP_3)]BF_4$	3/6	100	20	585	29	[11]
11	$RuCl_2(dppe)_2$	13/8.5	100	15.5	12900	830	[12]
12	$RuCl_2[P(CH_3)_3]_4$	13/8	50	64	3500	55	[13]
13	$RuCl_2\ (PMe_3)_4$	13/8	80	64	3500	55	[14]
14	$RhCl\ (PPh_3)_3$	4.8/6.4	100	5	125	25	[15]
15	$HCO_2W(CO)_5^-$	1.7/1.7	125	24	16.4	0.68	[16]
16	$HRu_3(CO)_{11}^-$	1.7/1.7	125	24	106	4.42	[17]
17	$HFe_3(CO)_{11}^-$	2/2	175	96	5.8	0.06	[18]
18	$Pd(diphos)_2$	2.5/2.5	140	21	33	1.57	[19]
19	**Ir/POP-Phen**	**4/6**	**160**	**48**	**138216**	**2280**	**this work**

Supplementary Table 2. Reaction performance comparison between the previously reported heterogeneous catalysts and the Ir/POP-Phen catalyst

Entry	**Cat.**	**CO_2/H_2 (MPa)**	**T (°C)**	**t (h)**	**TON**	**TOF (h^{-1})**	**Ref.**
1	Au-ZrO_2-9.0	8/8	200	1.0	534	534	[20]
2	Ru/N-Me-3-bpp-POP	2/6	160	4.0	1877	469	[21]
3	Ru@pDPPE	2/6	160	12	3401	283	[22]
4	Ag/ZrO_2	13/13	180	-	-	29.1	[23]
5	Ir-CTF	13/13	180	-	-	3.03	[24]
6	Cu/ZnO/Al_2O_3	14/2	150	0.33	13.4	43.6	[25]
7	Pd/Cu/ZnO	1/5	150	25	954	38.15	[26]
8	Hybrid-Gel RuMe-1	13/8.5	100	64	3180	50	[27]
9	**Ir/POP-Phen**	**4/6**	**160**	**48**	**138216**	**2280**	**this work**

6. Catalyst characterization

N_2 adsorption-desorption analysis

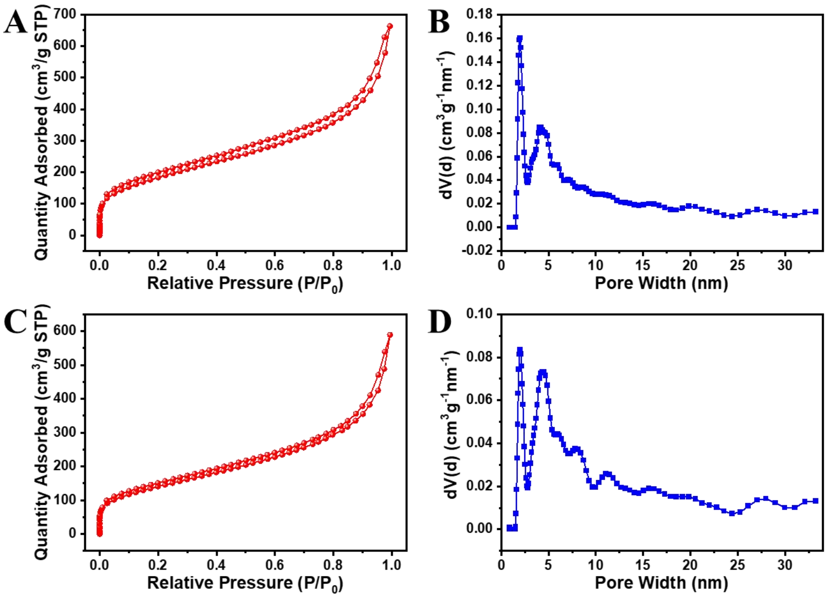

Supplementary Figure 1. N_2 adsorption-desorption isotherm and pore size distribution of the POP-Phen (A and B) and the spent Ir/POP-Phen (C and D).

Supplementary Table 3. The physical properties of the POP-Phen catalysts

Entry	**Catalyst**	**SA (m^2g^{-1})**[a]	**APD (nm)**[a]	**PV ($cm^{-3}g^{-1}$)**[a]
1	POP-Phen	659.542	6.224	1.026
2	Ir/POP-Phen	455.482	7.831	0.892
3	Ir/POP-Phen-spent	508.694	7.162	0.911

[a] Determined by an IQ_2 automated gas sorption analyzer. SA: BET surface area; APD: average pore diameter; PV: pore volume.

Scanning electron micrographs

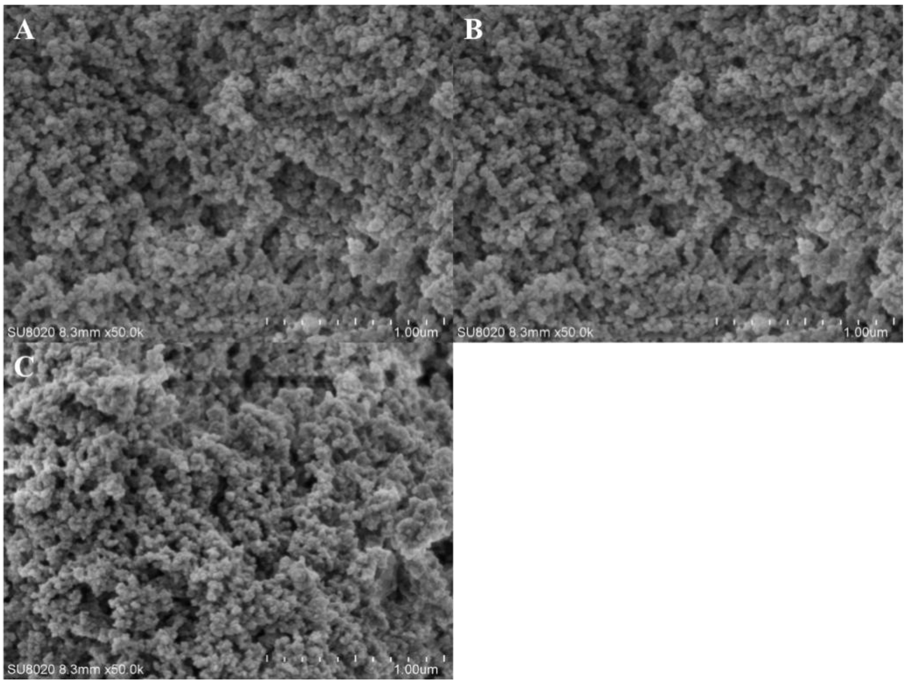

Supplementary Figure 2. SEM images of the POP-Phen (A), Ir/POP-Phen (B) and Ir/POP-Phen-spent (C).

TEM image of the Ir/POP-Phen.

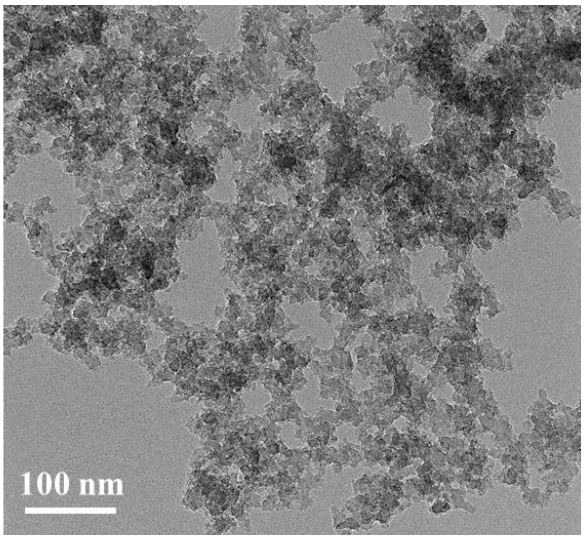

Supplementary Figure 3. TEM image of the Ir/POP-Phen.

CO absorbed FT-IR spectra.

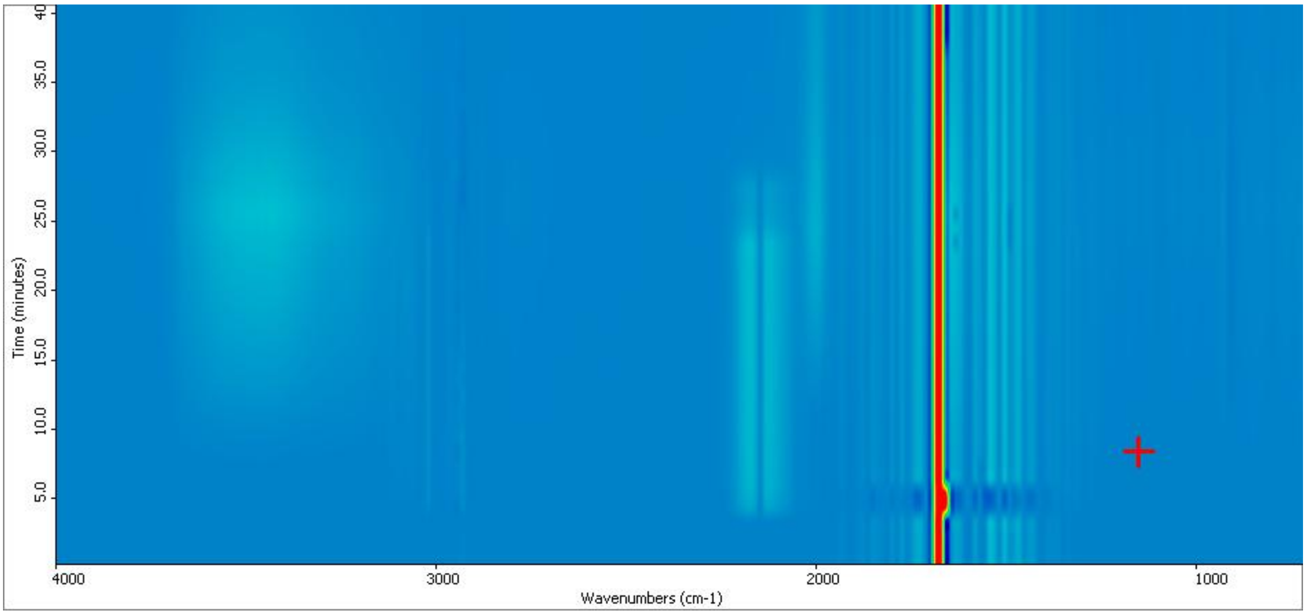

Supplementary Figure 4. CO absorbed FT-IR spectra of the Ir/POP-Phen.

TEM images of the Ir/POP-Phen-spent.

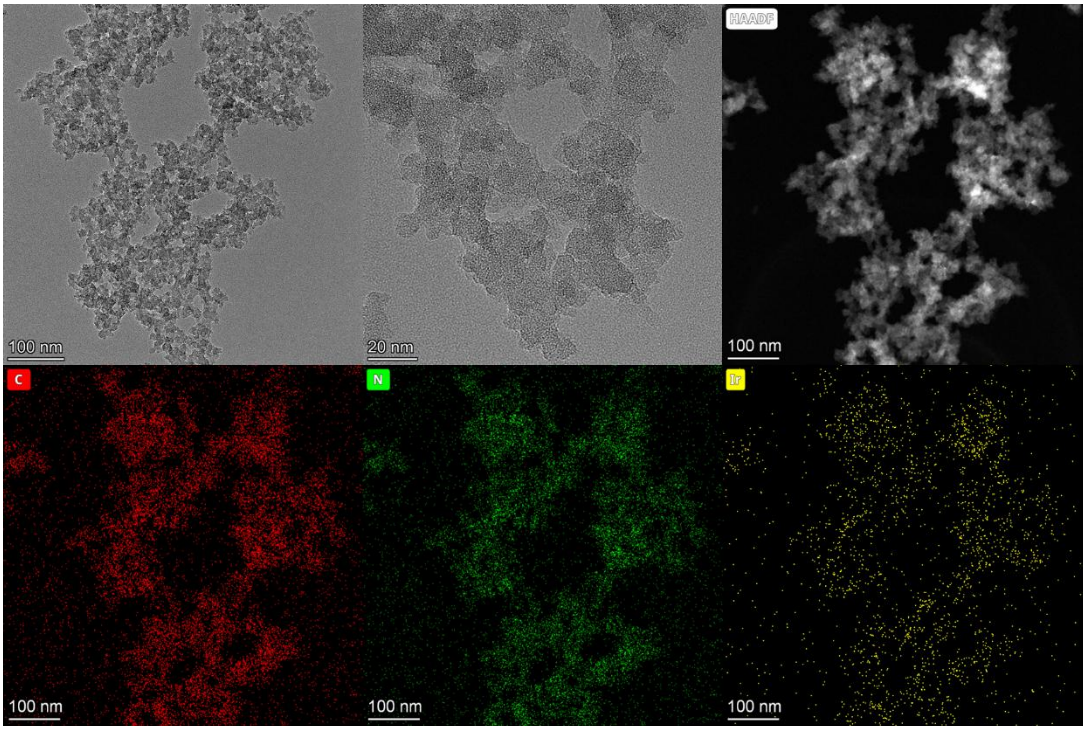

Supplementary Figure 5. TEM images of the Ir/POP-Phen-spent.

Abreaction-corrected HAADF-STEM image

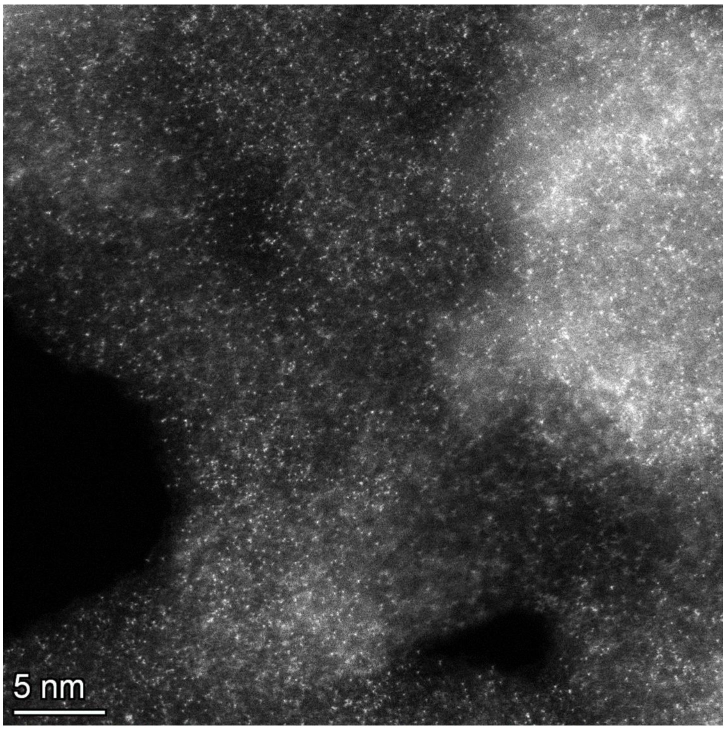

Supplementary Figure 6. Abreaction-corrected HAADF-STEM image of the Ir/POP-Phen-spent.

FT-EXAFS fitting analysis

Supplementary Table 4. EXAFS data fitting results of the Ir/POP-Phen

Sample	**Path**	**N**	**R (Å)**	**σ^2**	**E_0 (eV)**	**R**	**amp**
Ir/POP-Phen	Ir-N	4.12	2.04	0.00280	7.559	0.05007	0.67826
	Ir-Cl	2.16	2.35	0.00177	7.559	0.00771	0.67826

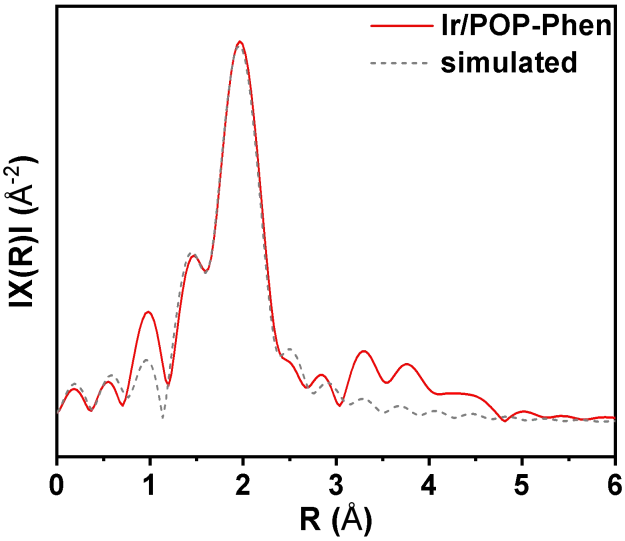

Supplementary Figure 7. FT-EXAFS fitting spectra of the Ir/POP-Phen.

7. Optimization of the reaction conditions

Supplementary Table 5. Screen of the M/POP-Phen catalysts[a]

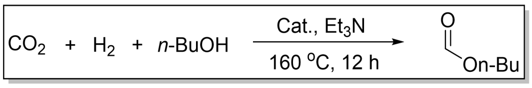

Entry	Cat.	Yield (mmol)	TON	TOF (h^{-1})
1	Pd/POP-Phen	1.25	1506	125
2	Rh/POP-Phen	0.51	614	52
3	Pt/POP-Phen	0.78	940	78
4	Au/POP-Phen	1.41	1699	142
5	Ru/POP-Phen	8.37	10084	841
6	Ir/POP-Phen	13.69	16494	1375
7	Cu/POP-Phen	1.22	1470	123
8	Co/POP-Phen	1.77	2133	178
9	Ag/POP-Phen	1.58	1904	159
10	Ni/POP-Phen	0.46	554	46

[a] Reaction conditions: *n*-BuOH (48 mL, 524 mmol), total pressure (10 MPa) of CO_2 and H_2 (CO_2 : H_2 = 4 : 6), Ir dosage (0.83 μmol), Et_3N (20 mL), reacted at 160 °C for 12 h. Yield, TON, and TOF were determined by GC analysis using *m*-xylene as the internal standard.

Supplementary Table 6. Ir contents in the catalysts and the filtration after each cycle, and the corresponding reaction performance [a]

Entry	**Recycling**	**Ir contents in the catalysts (wt.%)**	**Ir contents in the filtration (ppm)**	**Yield (mmol)** [b]	**TON** [b]	**TOF (h^{-1})** [b]
1	The fresh catalyst	8.30	-	-	-	-
2	The 1st run	8.26	<0.1 ppm	16.9	1016	85
3	The 2nd run	8.13	<0.1 ppm	16.8	1010	84
4	The 3rd run	8.28	<0.1 ppm	16.8	1013	84
5	The 4th run	8.31	<0.1 ppm	16.6	998	83

[a] Ir content was determined by ICP-AES. [b] Reaction conditions: *n*-BuOH (48 mL, 524 mmol), total pressure (10 MPa) of CO_2 and H_2 (CO_2: H_2 = 4: 6), Ir dosage (16.6 μmol), Et_3N (20 mL), reacted at 160 °C for 12 h. Yield, TON, and TOF were determined by GC analysis using *m*-xylene as the internal standard.

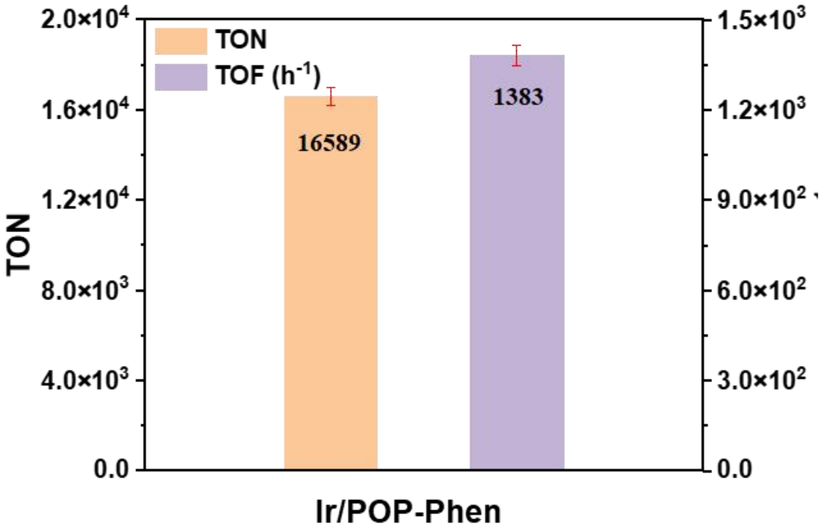

Supplementary Figure 8. Reductive O-formylation of carbon dioxide and *n*-BuOH via the Ir/POP-Phen. Reaction conditions: *n*-BuOH (48 mL, 524 mmol), total pressure (10 MPa) of CO_2 and H_2 ($CO_2 : H_2 = 4 : 6$), Ir dosage (0.83 μmol), Et_3N (20 mL), reacted at 160 °C for 12 h. Yield, TON, and TOF were determined by GC analysis using *m*-xylene as the internal standard.

8. Copies of quantitative GC and NMR spectra

NMR spectra of the ligands

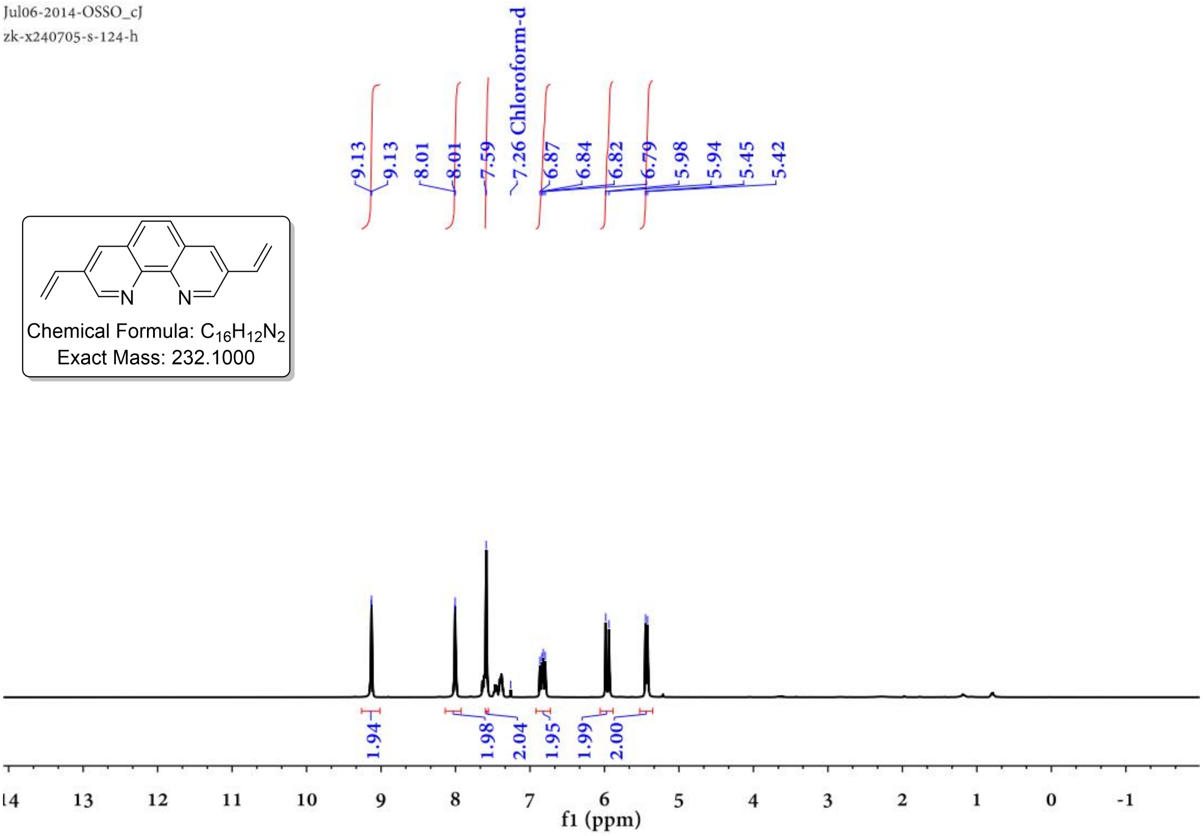

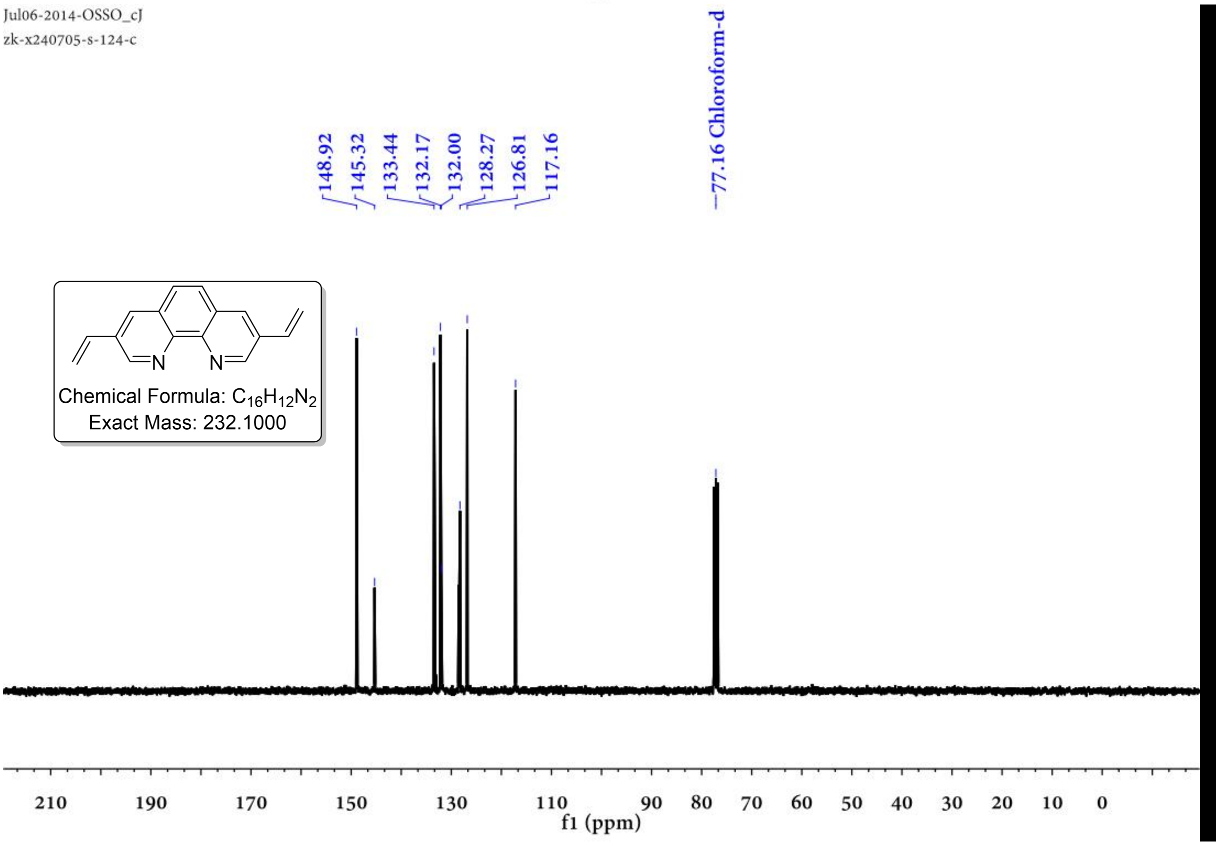

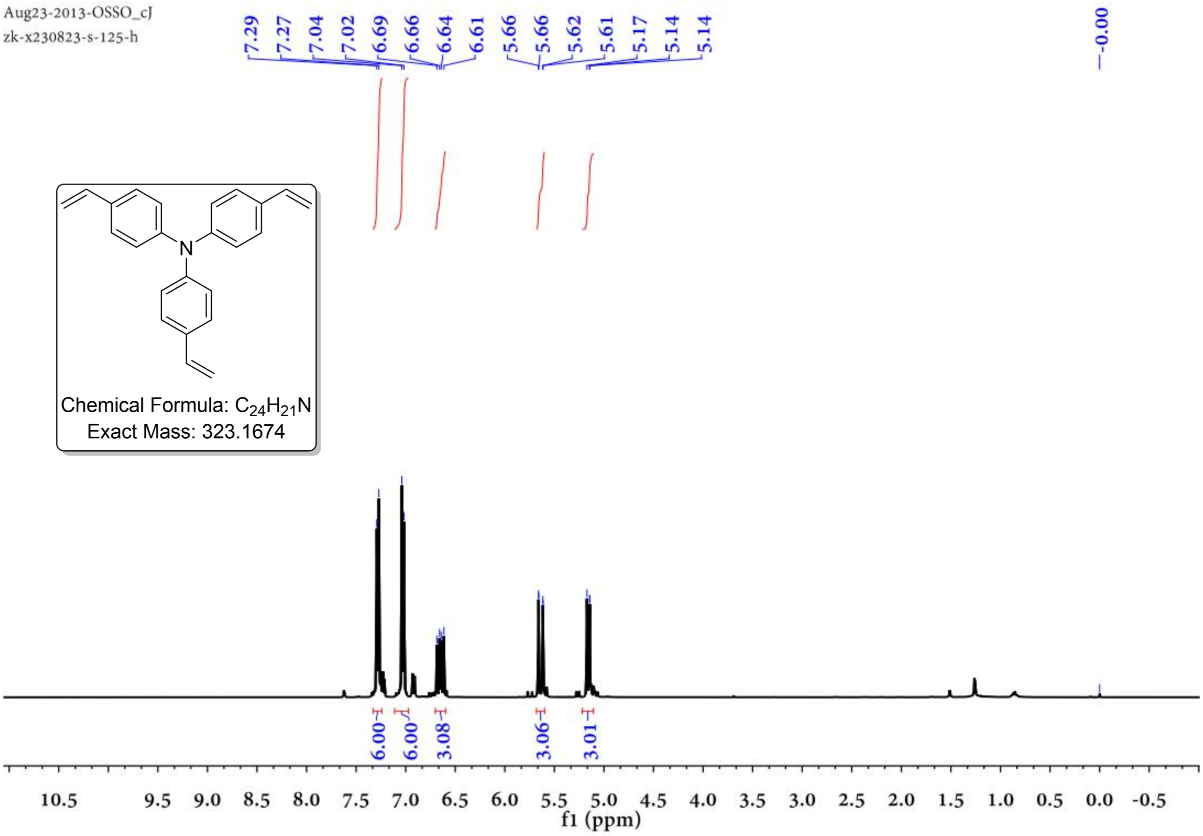
Aug23-2013-OSSO_cJ
zk-x230823-s-125-h
7.29
7.27
7.04
7.02
6.69
6.66
6.64
6.61
5.66
5.66
5.62
5.61
5.17
5.14
5.14
-0.00
N
Chemical Formula: $C_{24}H_{21}N$
Exact Mass: 323.1674
6.00
6.00
3.08
3.06
3.01
10.5
9.5
9.0
8.5
8.0
7.5
7.0
6.5
6.0
5.5
5.0
4.5
4.0
3.5
3.0
2.5
2.0
1.5
1.0
0.5
0.0
-0.5
f1 (ppm)

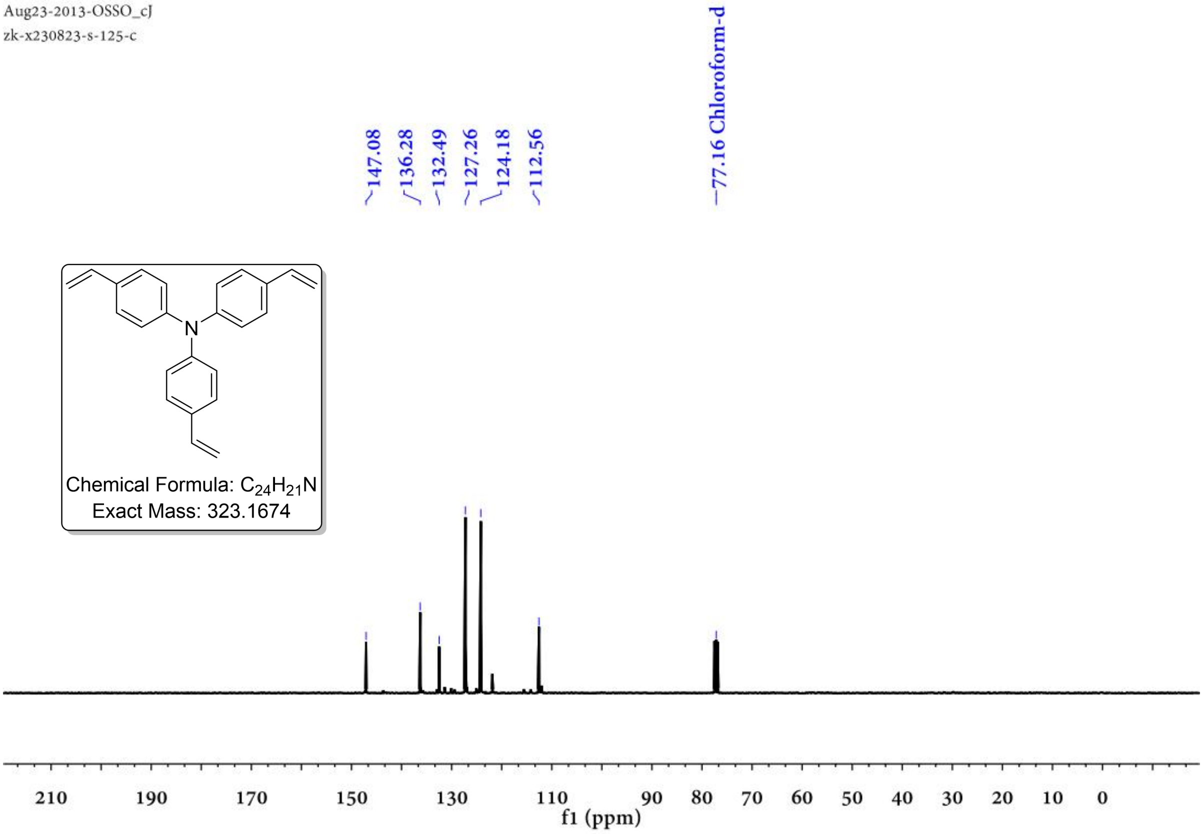
Aug23-2013-OSSO_cJ
zk-x230823-s-125-c
147.08
136.28
132.49
127.26
124.18
112.56
77.16 Chloroform-d
N
Chemical Formula: $C_{24}H_{21}N$
Exact Mass: 323.1674
210
190
170
150
130
110
90
80
70
60
50
40
30
20
10
0
f1 (ppm)

Quantitative GC spectra for O-formylation of *n*-BuOH

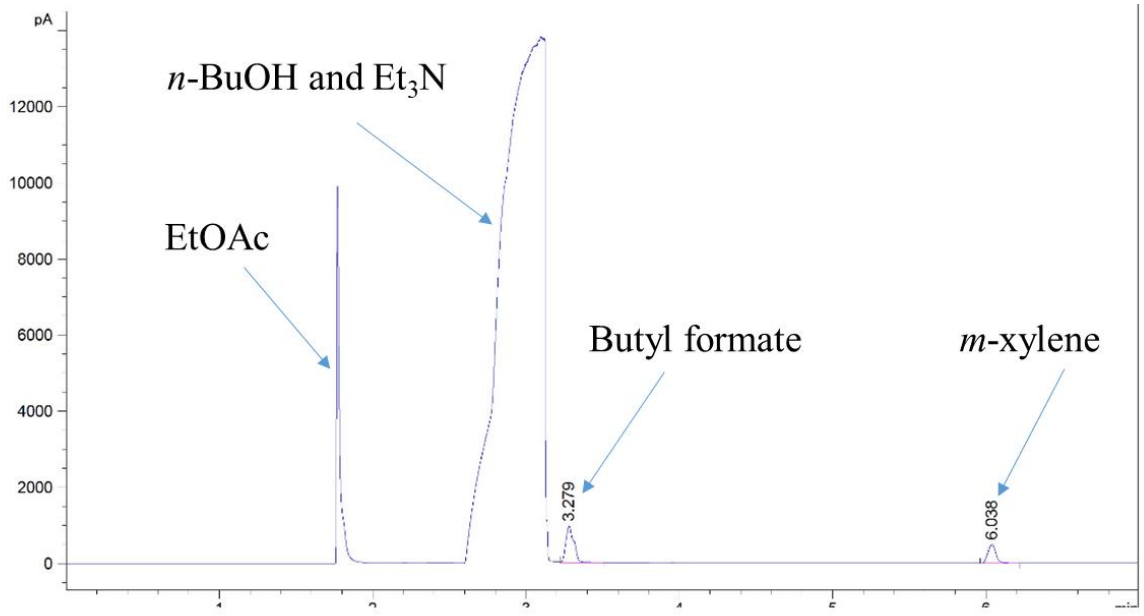

Peak No.	Ret. time	Area	Area%
1	3.279	3543.629	66.389
2	6.038	1794.220	33.613
Total		5377.849	10.002

Quantitative GC spectra for O-formylation of MeOH

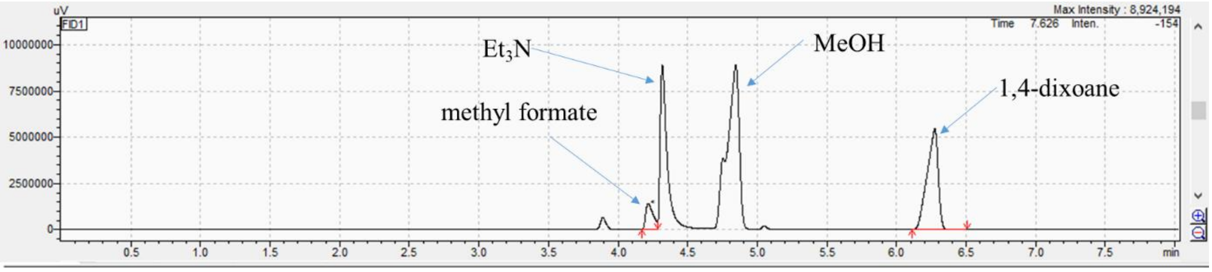

Peak No.	Ret. time	Area	Area%
1	4.216	5416204	15.179
2	6.274	30266320	84.821
Total		35682524	10.000

Quantitative NMR spectra for O-formylation of other alcohols

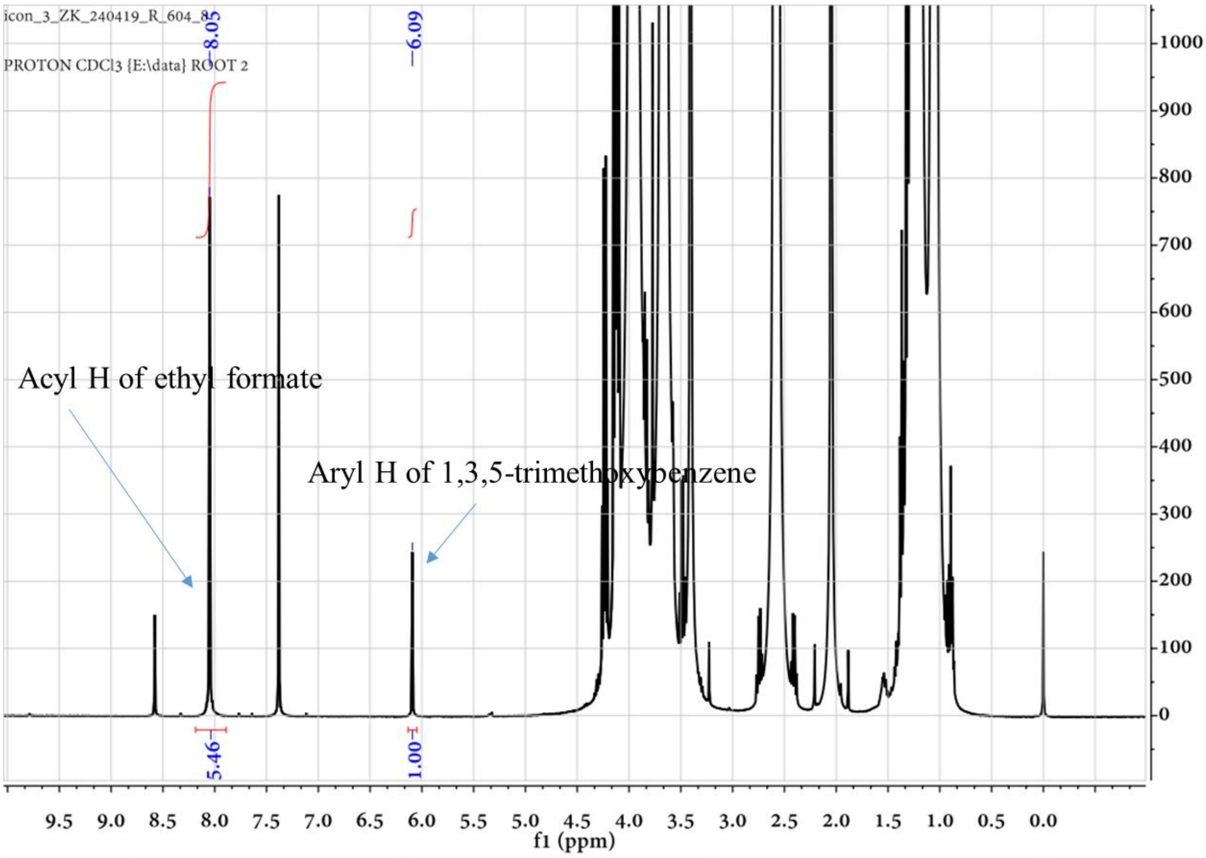

Chemical shift (ppm)	Area	Ethyl formate (mmol)
6.09	1.00	
8.05	5.46	33.28

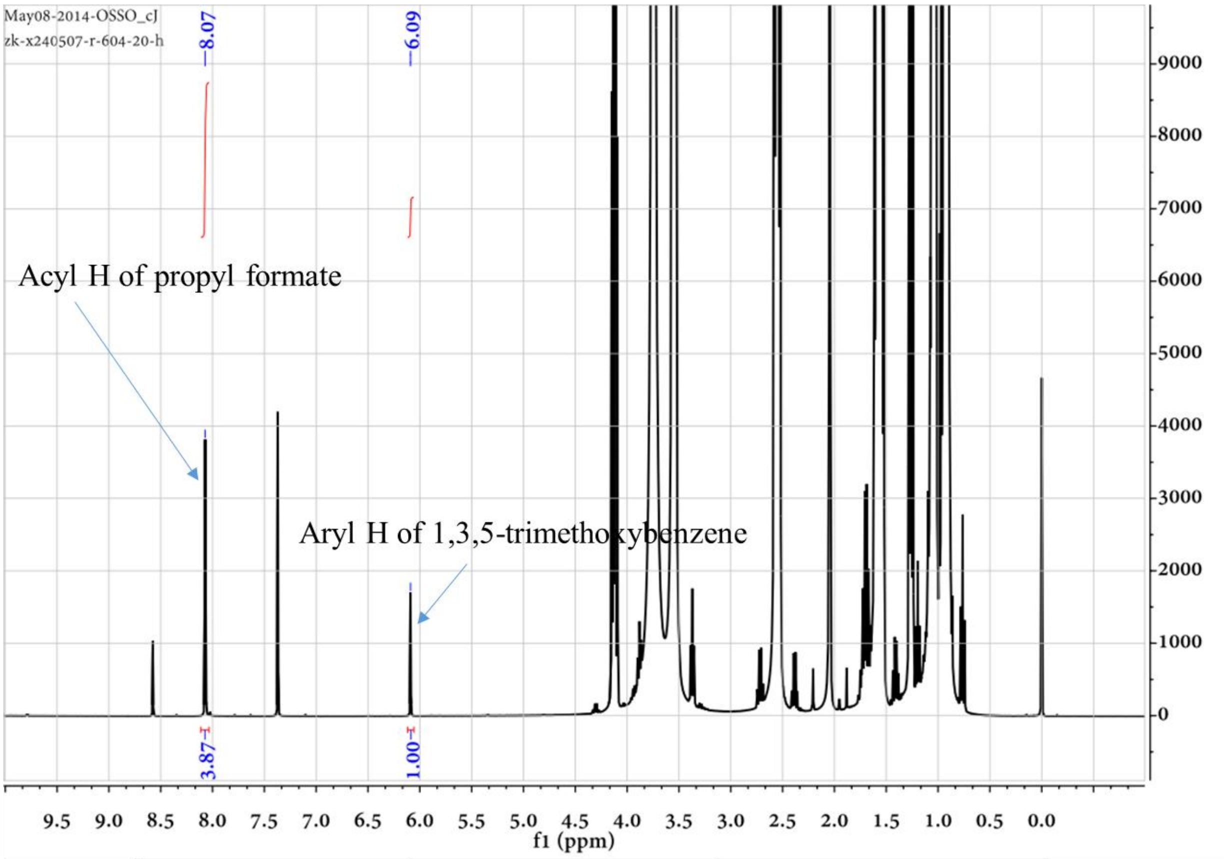

Chemical shift (ppm)	Area	Propyl formate (mmol)
6.09	1.00	
8.07	3.87	17.31

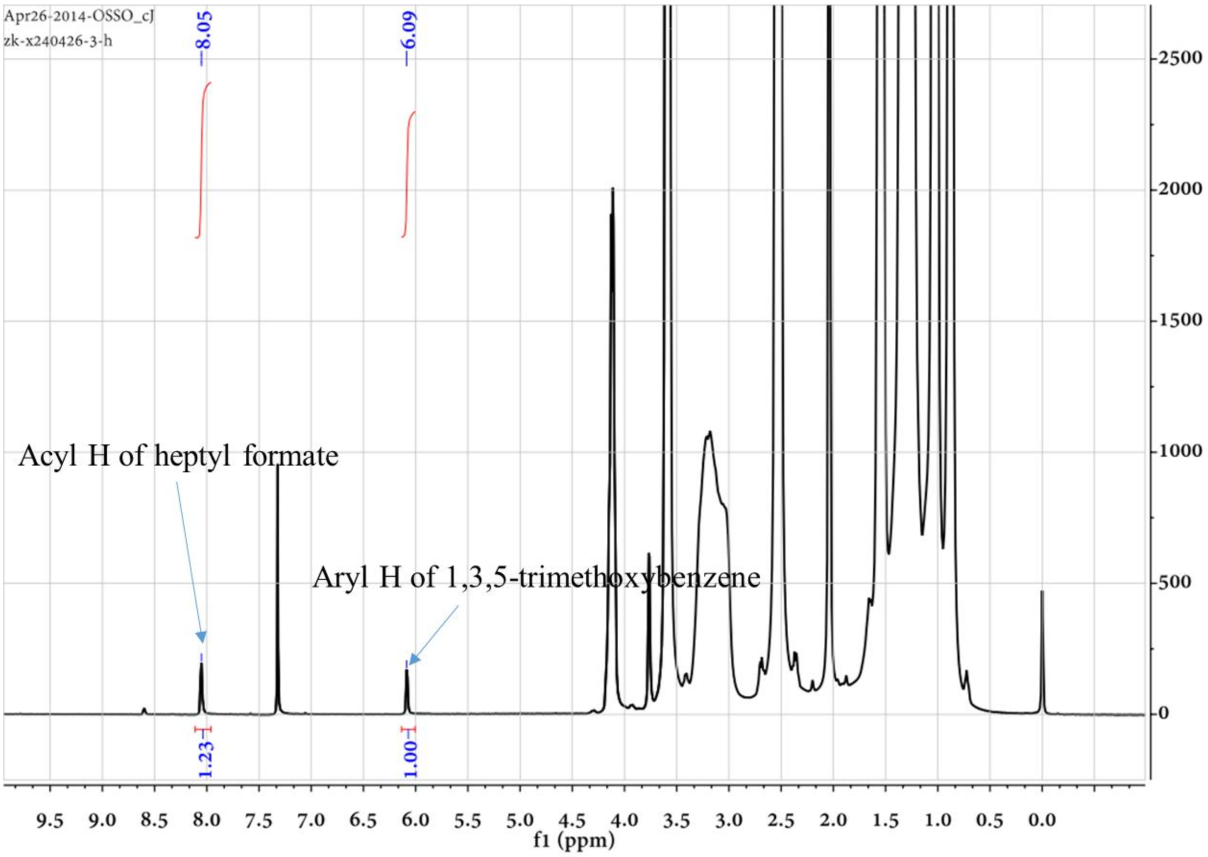

Chemical shift (ppm)	Area	Heptyl formate (mmol)
6.09	1.00	
8.05	1.23	6.33

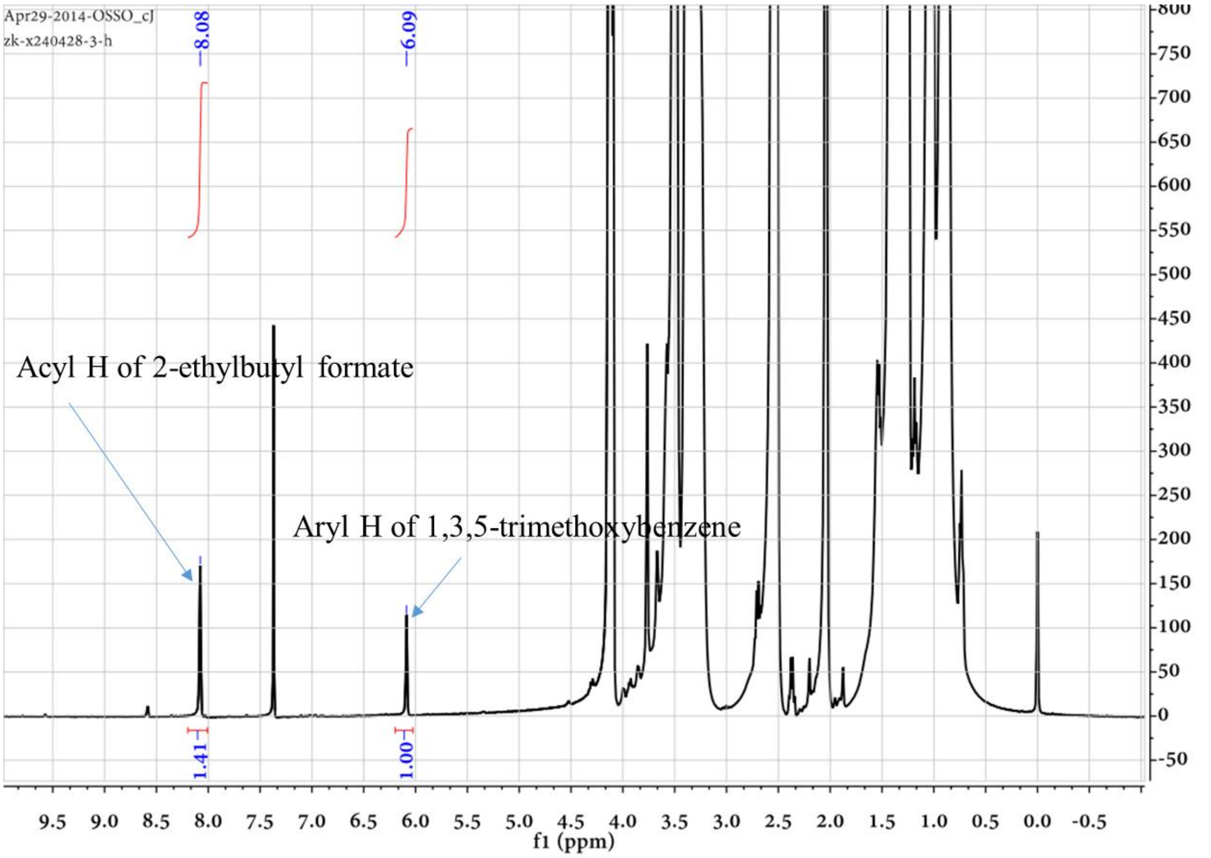

Chemical shift (ppm)	Area	2-Ethylbutyl formate (mmol)
6.09	1.00	
8.08	1.41	7.11

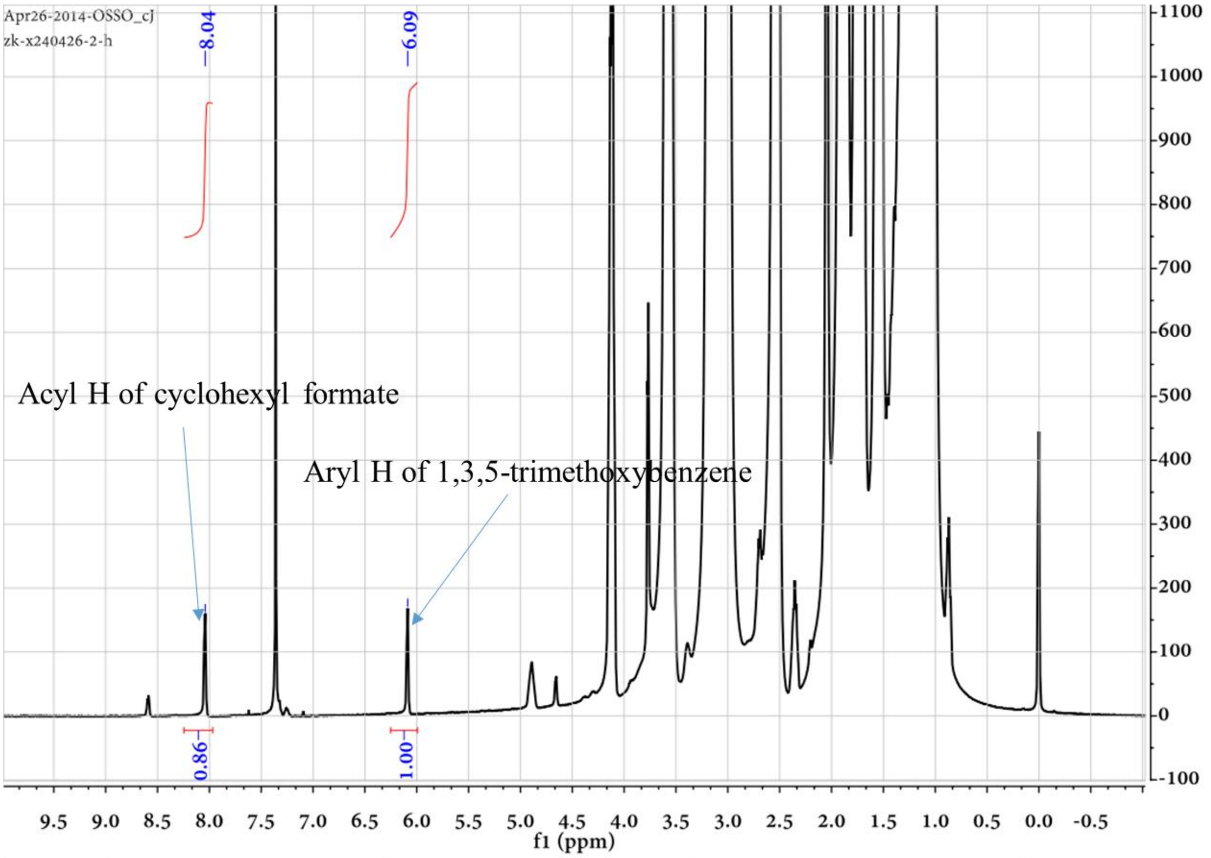

Chemical shift (ppm)	Area	Cyclohexyl formate (mmol)
6.09	1.00	
8.04	0.86	5.35

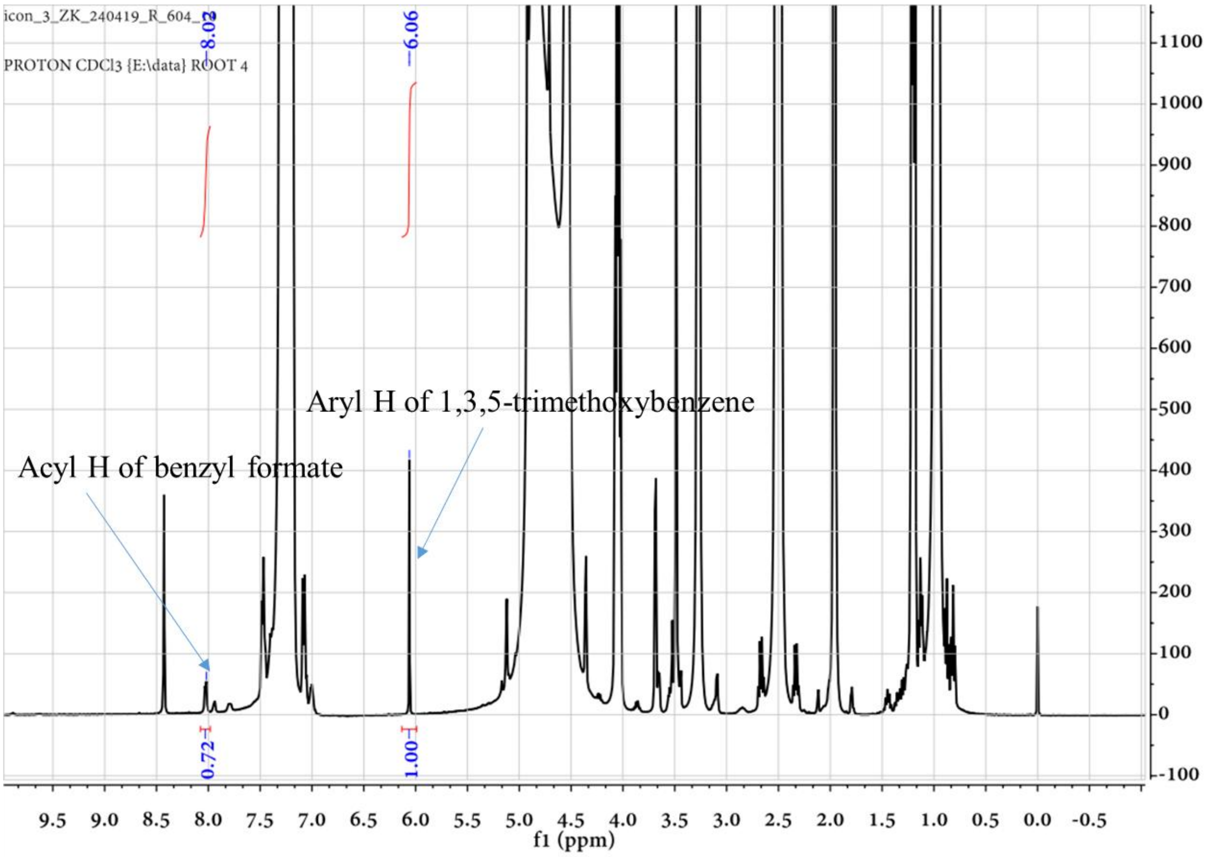

Chemical shift (ppm)	Area	Benzyl formate (mmol)
6.06	1.00	
8.02	0.72	5.35

9. References

1. Tang, Y.; Dai, Z.; Wang, S.; Chen, F.; Meng, X.; Xiao, F. S., Metalated Porous Phenanthroline-Based Polymers as Efficient Heterogeneous Catalysts for Regioselective C−H Activation of Heteroarenes. *Chem. - Asian J.* **2021,** *16*, 2469-2474.
2. Lemmens, V.; Vanbergen, T.; O'Rourke, G.; Marquez, C.; De Vos, D. E., Cascade Catalysis for the Hydrogenation of Carbon Dioxide to Methyl Formate Using a Molecular Ru-Phosphine Complex and the Metal-Organic Framework UiO-66 as Heterogeneous Acid. *ACS Appl. Energy Mater.* **2023,** *6*, 9153-9158.
3. Scott, M.; Westhues, C. G.; Kaiser, T.; Baums, J. C.; Jupke, A.; Franciò, G.; Leitner, W., Methylformate from CO2: an integrated process combining catalytic hydrogenation and reactive distillation. *Green Chem.* **2019,** *21*, 6307-6317.
4. Siebert, M.; Seibicke, M.; Siegle, A. F.; Kräh, S.; Trapp, O., Selective Ruthenium-Catalyzed Transformation of Carbon Dioxide: An Alternative Approach toward Formaldehyde. *J. Am. Chem. Soc.* **2018,** *141*, 334-341.
5. Westhues, N.; Belleflamme, M.; Klankermayer, J., Base-Free Hydrogenation of Carbon Dioxide to Methyl Formate with a Molecular Ruthenium-Phosphine Catalyst. *ChemCatChem* **2019,** *11*, 5269-5274.
6. Yadav, M.; Linehan, J. C.; Karkamkar, A. J.; van der Eide, E.; Heldebrant, D. J., Homogeneous Hydrogenation of CO2 to Methyl Formate Utilizing Switchable Ionic Liquids. *Inorg. Chem.* **2014,** *53*, 9849-9854.
7. Gowrisankar, S.; Federsel, C.; Neumann, H.; Ziebart, C.; Jackstell, R.; Spannenberg, A.; Beller, M., Synthesis of stable phosphomide ligands and their use in Ru-catalyzed hydrogenations of bicarbonate and related substrates. *ChemSusChem* **2013,** *6*, 85-91.
8. Ziebart, C.; Federsel, C.; Anbarasan, P.; Jackstell, R.; Baumann, W.; Spannenberg, A.; Beller, M., Well-Defined Iron Catalyst for Improved Hydrogenation of Carbon Dioxide and Bicarbonate. *J. Am. Chem. Soc.* **2012,** *134*, 20701-20704.
9. Federsel, C.; Ziebart, C.; Jackstell, R.; Baumann, W.; Beller, M., Catalytic hydrogenation of carbon dioxide and bicarbonates with a well-defined cobalt dihydrogen complex. *Chem. - Eur. J.* **2012,** *18*, 72-5.
10. Huff, C. A.; Sanford, M. S., Cascade Catalysis for the Homogeneous Hydrogenation of CO2 to Methanol. *J. Am. Chem. Soc.* **2011,** *133*, 18122-18125.
11. Federsel, C.; Boddien, A.; Jackstell, R.; Jennerjahn, R.; Dyson, P. J.; Scopelliti, R.; Laurenczy, G.; Beller, M., A well-defined iron catalyst for the reduction of bicarbonates and carbon dioxide to formates, alkyl formates, and formamides. *Angew. Chem., Int. Ed.* **2010,** *49*, 9777-80.

12. Kröcher, O.; A. Köppel, R.; Baiker, A., Highly active ruthenium complexes with bidentate phosphine ligands for the solvent-free catalytic synthesis of N,N-dimethylformamide and methyl formate. *Chem. Commun.* **1997,** *33*, 453-454.

13. Jessop, P. G.; Hsiao, Y.; Ikariya, T.; Noyori, R., Homogeneous Catalysis in Supercritical Fluids: Hydrogenation of Supercritical Carbon Dioxide to Formic Acid, Alkyl Formates, and Formamides. *J. Am. Chem. Soc.* **1996,** *118*, 344-355.

14. Jessop, P. G.; Hsiao, Y.; Ikariya, T.; Noyori, R., Methyl Formate Synthesis by Hydrogenation of Supercritical Carbon-Dioxide in the Presence of Methanol. *J. Chem. Soc., Chem. Commun.* **1995**, 707-708.

15. Phala, H.; Kudo, K.; Mori, S.; Sugita, N., Tris (triphenylphosphine) rhodium(I) Chloride Catalyzed Synthesis of Methyl Formate from Methanol, Carbon Dioxide and Hydrogen in the Presence of a Tertiary Amine (Commemoration Issue Dedicated to Professor Eiichi Fujita on the Occasion of his Retirement). *Bull. Inst. Chem. Res., Kyoto Univ.* **1985,** *63*, 63-71.

16. Darensbourg, D. J.; Ovalles, C., Anionic Group 6B metal carbonyls as homogeneous catalysts for carbon dioxide/hydrogen activation. The production of alkyl formates. *J. Am. Chem. Soc.* **1984,** *106*, 3750-3754.

17. Darensbourg, D. J.; Ovalles, C.; Pala, M., Homogeneous catalysts for carbon dioxide/hydrogen activation. Alkyl formate production using anionic ruthenium carbonyl clusters as catalysts. *J. Am. Chem. Soc.* **1983,** *105*, 5937-5939.

18. Evans, G. O.; Newell, C. J., Conversion of CO2, H2, and alcohols into formate esters using anionic iron carbonyl hydrides. *Inorg. Chim. Acta* **1978,** *31*, L387-L389.

19. Inoue, Y.; Sasaki, Y.; Hashimoto, H., Synthesis of formates from alcohols, carbon dioxide, and hydrogen catalysed by a combination of group VIII transition-metal complexes and tertiary amines. *J. Chem. Soc., Chem. Commun.* **1975**, 718-719.

20. Wu, C.; Zhang, Z.; Zhu, Q.; Han, H.; Yang, Y.; Han, B., Highly efficient hydrogenation of carbon dioxide to methyl formate over supported gold catalysts. *Green Chem.* **2015,** *17*, 1467-1472.

21. Park, H.; Park, K.; Jung, K.-D.; Yoon, S., CO2 hydrogenation into formate and methyl formate using Ru molecular catalysts supported on NNN pincer porous organic polymers. *Inorg. Chem. Front.* **2021,** *8*, 1727-1735.

22. Sun, R.; Kann, A.; Hartmann, H.; Besmehn, A.; Hausoul, P. J. C.; Palkovits, R., Direct Synthesis of Methyl Formate from CO2 With Phosphine-Based Polymer-Bound Ru Catalysts. *ChemSusChem* **2019,** *12*, 3278-3285.

23. Corral-Pérez, J. J.; Copéret, C.; Urakawa, A., Lewis acidic supports promote the selective hydrogenation of carbon dioxide to methyl formate in the presence of methanol over Ag catalysts. *J.*

Catal. **2019,** *380*, 153-160.

24. Corral-Pérez, J. J.; Billings, A.; Stoian, D.; Urakawa, A., Continuous Hydrogenation of Carbon Dioxide to Formic Acid and Methyl Formate by a Molecular Iridium Complex Stably Heterogenized on a Covalent Triazine Framework. *ChemCatChem* **2019,** *11*, 4725-4730.

25. Kerry Yu, K. M.; Tsang, S. C., A Study of Methyl Formate Production from Carbon Dioxide Hydrogenation in Methanol over a Copper Zinc Oxide Catalyst. *Catal. Lett.* **2011,** *141*, 259-265.

26. Yu, K. M. K.; Yeung, C. M. Y.; Tsang, S. C., Carbon Dioxide Fixation into Chemicals (Methyl Formate) at High Yields by Surface Coupling over a Pd/Cu/ZnO Nanocatalyst. *J. Am. Chem. Soc.* **2007,** *129*, 6360-6361.

27. Krocher, O.; Koppel, R. A.; Froba, M.; Baiker, A., Silica hybrid gel catalysts containing Group(VIII) transition metal complexes: Preparation, structural, and catalytic properties in the synthesis of N,N-dimethylformamide and methyl formate from supercritical carbon dioxide. *J. Catal.* **1998,** *178*, 284-298.